

A computational model of the integration of landmarks and motion in the insect central complex

Praneet Vibhu Balabolu*

Department of Electrical Engineering
Columbia University
New York, NY, USA
pb2735@columbia.edu

Aditya Sinha*

Department of Electrical Engineering
Columbia University
New York, NY, USA
as5624@columbia.edu

Abstract—Research has shown that the insect central complex (CX) might be responsible for many behaviours related to locomotion and vision. One of the experiments conducted revealed a form of neural compass i.e., neural activity corresponding to the animal’s orientation, in the CX of the fruit fly’s brain. The model proposed in this work combines both angular velocity and angular position measurements to pinpoint the orientation of the model with respect to the virtual arena. It further shows that using both of these measures improves tracking as compared to a single measure. Studying such a model can inspire approaches towards design of fully autonomous robots. This work tries to replicate the results of [1]

Index Terms—insect central complex, fruit fly, neural compass

I. INTRODUCTION

As is the case with most insect species, the fruit fly has a central complex (CX) at the center of its brain. It has been observed that most sensory inputs converge at the CX, and its activity seems to influence behaviours such as locomotion, visual pattern memory and visual place learning. This paper explores the structure of one set of neurons (Ellipsoid body) in the CX responsible for the neural compass activity and creates a constrained computational model which imbibes the CX functionality. The activity of the neural compass could be underlying more complex locomotory behaviours and modelling this neural activity could help us identify the mechanisms behind them.

The most notable of recent experiments are those performed by Seelig and Jayaraman [2] on restrained flies waking on a rotating air-supported ball in a virtual arena. They demonstrated that the ellipsoid body (EB) neurons tracked the location of a landmark through a bump of neural activity. They also showed that the EB bump is likely driven by positional processes or motion-based processes with the positional process being more effective. The evidence for angular motion detection was provided by experiments in which the stimuli was regular grating with no landmarks. The fly was still able to orient itself based on angular motion integration but required an operable CX to function. Two possible angular motion measures that were considered were optomotor response and angular velocity response. Optomotor response is formed by simple correlation

detectors, but is unsuitable for angular motion integration because it depends on the frequency of contrasting edges passing through, and hence dependent on spatial frequency. Therefore, it would be inconsistent in its response to a given rotation. Angular velocity response, on the other hand, scales with the angular velocity independent of spatial frequency and contrast, and hence is used in this model to drive the angular motion integration. This model addresses the effectiveness of combining angular motion integration and positional cues in tracking orientation and the advantages of having both the systems.

II. TECHNICAL APPROACH

A. Visual Detection

We use an array of 24 horizontal by 1 vertical ommatidia per eye in a grid to track the orientation only in the horizontal space. We assume that this 48 by 1 grid covers the whole 360° field of view. The positional responses are obtained by summation of the the responses over small regions of the visual field. In this case, we used the intensities of the field of view of each ommatidia to determine its response. The 360° field of view is divided into 16 regions of 22.5° width each for the positional input calculation.

To obtain the motion detection response, we use the model based on [3] to construct two Angular Velocity Detecting Units (AVDUs) (Fig. 1), one preferring progressive and the other preferring regressive flight. The angular velocity needs to be processed through differential operations across the ommatidial grid, and so we make use of the Hassenstein-Reichardt correlation detector. A pair of HR detectors with different but known time constants are connected to each pair of ommatidia, with one preferring forward direction and one preferring the backward direction. It is to be noted that the input given to these HR detectors is the response of the photoreceptors, which are implemented as edge detectors to find salient features in motion. The angular velocity detector units sum up the correlation detector responses across both the eyes giving two final inputs one each for progressive and regressive directions and whose magnitude scales with the angular velocity. The progressive and regressive responses also inhibit each other to allow driving only in one direction.

*Both authors contributed equally to this manuscript

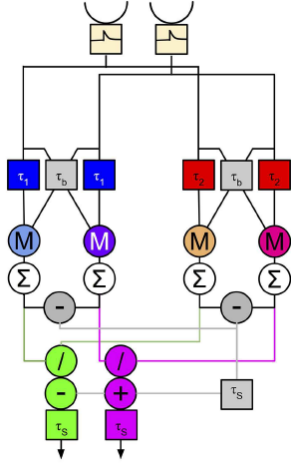


Fig. 1. Angular Velocity Detector Unit

B. Ring Attractor Network

The ring attractor network in our model is a direct parallel of the structure present in the ellipsoid body present in the fly brain ([2], [4]). The ring attractor is divided into 16 wedges, each having a neuron, with each neuron connected to the next one to form a ring. The ring attractor neurons have inhibitory and excitatory connections such that the neural activity is similar to a bump. The inhibitory connections are all to all to keep the network stable. The excitatory connections on the other hand are only to the 4 closest neurons and the neuron itself. The weights are chosen to resemble a Gaussian distribution which would ensure a single bump with a full value half width as measured by [2]. Apart from the main ring attractor, the EB also has other such concentric rings and interconnections between the rings. In our model, these structures are also present as positional input neurons (receiving landmark input features) and two rings of rotational neurons. Apart from these, there are two driver neurons that drive the ring by modulating the strength of the rotational neurons. These receive motion detection information in the form of the AVDU outputs. All neurons used are graded potential Leaky Integrators and all synapses are simple weights. Implementation-wise, even the rotational neurons are considered to be modulatory synapse nodes in the network graph. The complete ring neuron dynamics is as follows.

$$\frac{dr_i}{dt} = \frac{-r_i + E_i^r + I^r + w_p p_i + c_{i-1} + a_{i+1}}{\tau_r}$$

$$E_i^r = 0.6r_i + 0.35(r_{(i+1)} + r_{(i+1)}) + 0.225(r_{(i+2)} + r_{(i+2)})$$

$$I^r = -0.1 \sum_0^{i_{max}} r_i$$

$$a_i = d_a r_i$$

$$c_i = d_c r_i$$

The detailed connectivity of this ring attractor network is as shown in Fig. 2. All 16 positional neurons are connected to the 16 ring neurons in a one-one fashion. Each rotational neuron ring is that the neurons in it take input from one ring neuron, have the weight modulated by the corresponding driver input and give it to the next neuron. The only difference is that the one ring getting input from one driver tries to drive the neuronal activities in the ring clockwise while the other tries to drive it anticlockwise, thus indirectly creating a competition between the two driver inputs to decide direction of motion. The two driver neurons give output to all the neurons in their corresponding rotational ring, thus controlling the strength of rotation. Within the ring, each neuron gives local excitation to two of its neighbouring neurons on either side and to itself, with the weights being gaussian distributed. This ensures that the shape of the bump is gaussian, which is as observed in experiments in the fly brain. There are also $\binom{16}{2}$ inhibitory connections between all the neurons in the ring attractor to provide shaping of the bump and stability to the system when the bump travels on motion.

The combination of the landmark inputs through positional neurons and motion inputs through AVDU and rotational neurons results in an integration of both, and this is the core idea behind the working of this model. We probe outputs from the ring neurons and analyse the representation and calculate the azimuth from it.

C. Calculation of Azimuth

To map the position of the bump with the azimuth of the object, assume that the beginning of the sector represented by ring neuron, r_0 corresponds to angle 0° in the virtual arena. We consider unit vectors from the center of the ring to each of the ring neurons as our basis functions. The position of the object is obtained by weighting the activity of all ring neurons with the corresponding ring unit vectors. The azimuth is then found by calculating the angle between the initial position (the 0° vector in this case) and the weighted vector.

$$v_{sum} = \sum_{i=0}^{i_{max}} r_i v_i$$

$$\phi_{est} = \arccos(v_{sum} \cdot v_{init})$$

III. EXPERIMENTS & RESULTS

Our experimental setup assumes a single vertical bar rotating horizontally with a constant angular velocity. This is the reason why a horizontal detector array is sufficient to track this motion. The angular width of the bar is 11.5° . Our model is built and simulated using the Neurokernel framework defined in [5]

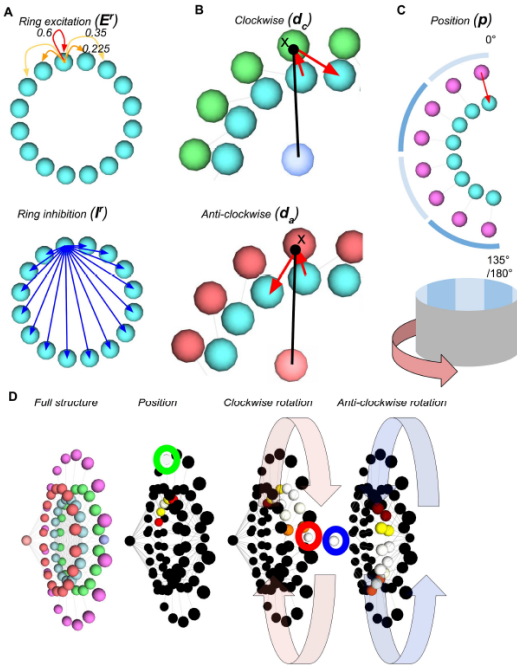


Fig. 2. Ring attractor circuit. A shows the local excitatory and inhibitory connections. B shows the neural circuit for rotating the bump of activity around the ring clockwise and anti-clockwise for a single pair of wedges. The activity is gated by the driver neuron which multiplies the ring activity to produce the output to the next wedge. C shows the positional input to the ring. D shows (left to right) the full structure of the ring; the ring being seeded by positional activity (green); the clockwise driver neuron (red); the anti-clockwise driver neuron (blue).

A. Visual Detector Optometric Response

We first tested the trend of the AVDU outputs to ensure that its response scales with the angular velocity. The input bar was rotated at different angular velocities and the response recorded of the AVDU pair was recorded as shown in Fig. 3. Depending on the direction of motion, we observe that output of one scales while the other is completely inhibited.

The other component of the optometric response given to the central complex (CX) are the 16 landmark features calculated as averages of broad receptive fields.

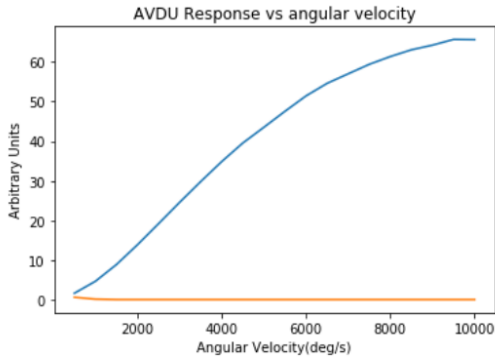


Fig. 3. AVDU response of both driver neurons with respect to angular velocity: blue is progressive and orange is regressive

B. Ring Attractor with Landmark Inputs

For seeing the effect of positional landmark inputs on the representation inside the CX, we set the driver input weights to be zero, effectively turning off the modulatory rotational neurons. Fig. 4 depicts the resulting outputs of the ring neurons, and we see that as the bar passes across the eye, different neurons get activated and there is a response which is not quite gaussian, but has a similar rising and falling structure due to the leaky integrators and excitations from the nearby neurons involved.

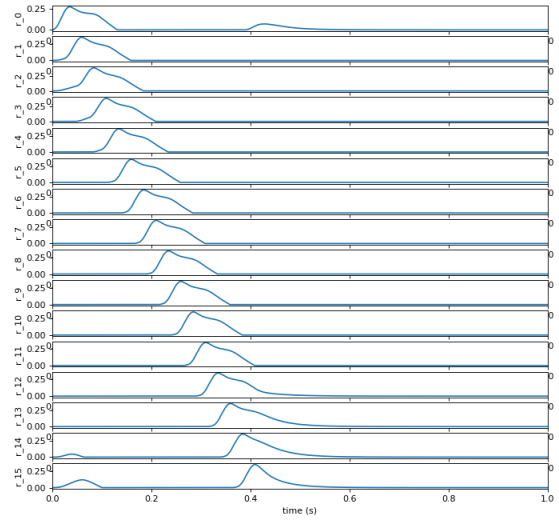


Fig. 4. Ring neuron responses for the system with only positional inputs over the time of simulation

C. Ring Attractor with Motion Inputs

To analyse the azimuth tracking by motion detection inputs, we use the modulatory input from the drivers (which in turn receive input from the AVDUs). The synapse weights from the positional neurons set to zero and we initialize one ring attractor neuron to allow the neuronal activity to flow through the ring. In Fig. 5, we see the motion information being encoded in the ring, and there is a gaussian like response both across time in a neuron, and across neurons at a single point in time (gives rise to the bump). Apart from giving us insight into the importance of motion detection in neural representation of objects in the CX, this experiment is also important to tune the time constant of the ring neurons, since they control how fast the bump moves on receiving input from the AVDU. Parameter tuning is done so that one rotation of the stimulus corresponds to one rotation of the bump in the ring, and so that there is no boosting in the response amplitudes as the activity travels through the ring.

D. Ring Attractor with Integration

When we use all 18 (16+2) inputs to the ring attractor network, we observe a response as shown in Fig. 6. It is worth noting that although the response is shaped like what we observe for the case of only AVDU (motion) inputs (and not

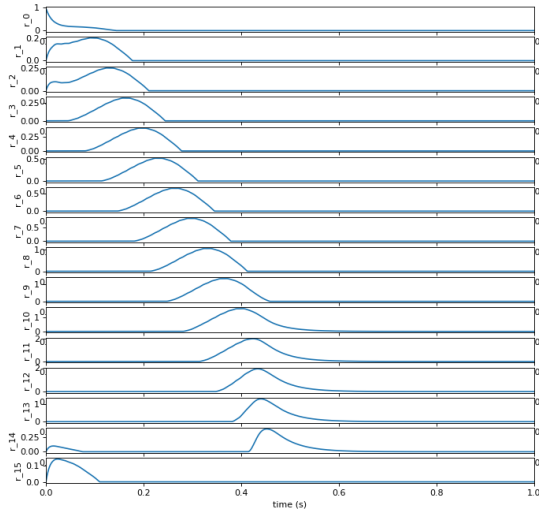


Fig. 5. Ring neuron responses for the system with only motion inputs over the time of simulation

raggedly like for landmark inputs), we have a lingering effect in response after the stimulus subsides that wasn't observed earlier when just the AVDU inputs were used. This is the effect of the positional landmark inputs that give weight to the neuronal activities of the ring depending on which region of the field is activated.

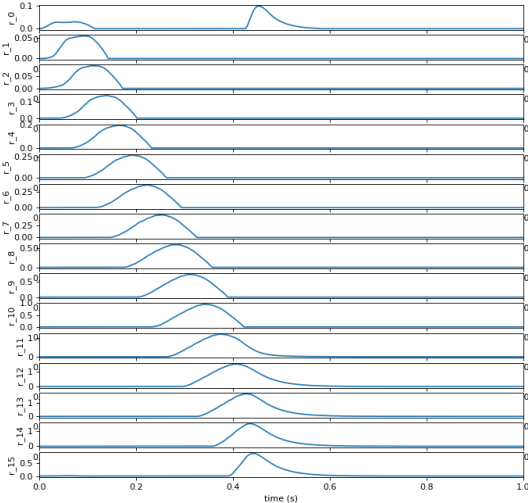


Fig. 6. Ring neuron responses for the integrated system over the time of simulation

We use the responses obtained to determine the azimuth estimated by our model using the method mentioned in Section II.C. The results shown in Fig. 7 compare the estimated azimuth using only landmarks, only motion and an integration of both. These are compared with the true azimuth of the rotating bar, and we observe that the integrated response tracks the azimuth slope and value much more accurately than the other two and motion performs the worst.

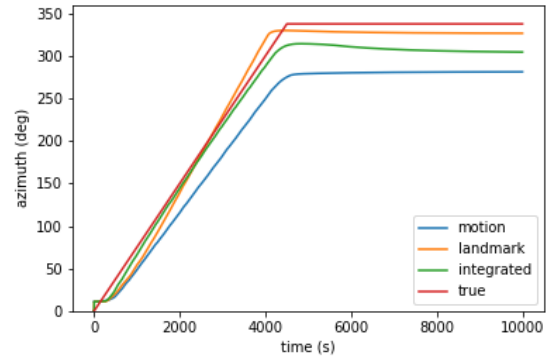


Fig. 7. Tracked azimuth with the different combinations combined with the ground truth

IV. DISCUSSION

From our simple example of a moving bar in one direction, we have shown the feasibility of the proposed model in explaining a lot of features of fly behaviour when it comes to visual landmark mapping and path integration. The bump noted in the experiments in [2] is also seen in our model, and it responds to landmark features as well as motion. It is also seen that landmark inputs give poor shaping of the bump whereas motion inputs decay quickly as soon as motion stops. It is an integration of these two that incorporates the best of both features, as is evident from the more accurate azimuth tracking.

It is worth noting that although we have put inhibitory connections throughout the ring for stability, the balance is very delicate and as the rotational neurons simply multiply the ring activities with the driver input, the problem of boosting is persistent and will eventually factor in for longer stimuli. This is one of the limitations of our model. Neurobiologically speaking, most systems in the brain comprise of spiking neurons and non-memoryless synapses. This inherent non-linearity is paramount in providing robustness to the system, and the fact that this model consists of only graded potentials and memoryless synapses is its major shortcoming.

A. Future Directions

Although the experiments we have run stand sufficient to argue for the importance of integration of landmark and motion inputs for representation in the central complex, the real nature and extent of how much each of the components contribute has been unexplored. To get an insight into this, we can consider providing stimuli that move non-uniformly: for example, a bar that moves, stops and then moves again or in another direction, stimuli that move with changing velocity, or even a stimulus with two bars, where only one is moving.

To make the model more robust, we would need to make major changes to it to replace the graded potential neurons with spiking ones. It would also be beneficial to use excitatory alpha synapses, inhibitory GABAB synapses and dopamine modulated synapses instead of the simple synapse models we have used. When tuned correctly with slight modifications in

the network architecture, this is expected to give better results that more closely resemble the behavior of the fly brain.

ACKNOWLEDGMENT

We would like to thank Prof. Aurel Lazar for teaching us about the details of canonical motion detection circuits in the fly brain and for giving us insight into the functioning of various neuropils in the central complex. We would also like to thank Mehmet Kerem Turkcan, our T.A. for the course, who has helped us with all the implementation details, working and data flow of neurodriver. Lastly, we would like to thank all the creators of the Neurokernel project for providing us with a platform to build and simulate circuits in the fly brain.

REFERENCES

- [1] Cope AJ, Sabo C, Vasilaki E, Barron AB, Marshall JAR (2017) A computational model of the integration of landmarks and motion in the insect central complex. PLOS ONE 12(2): e0172325. <https://doi.org/10.1371/journal.pone.0172325>
- [2] Seelig JD, Jayaraman V. Neural dynamics for landmark orientation and angular path integration. Nature. 2015; 521(7551):186191. doi: 10.1038/nature14446 PMID: 25971509
- [3] Cope A, Sabo C, Gurney KN, Vasilaki E, Marshall JAR. A Model for an Angular Velocity-Tuned Motion Detector Accounting for Deviations in the Corridor-Centering Response of the Bee. PLoS Comput Biol. 2016;. doi: 10.1371/journal.pcbi.1004887 PMID: 27148968
- [4] Turner-Evans DB, Jayaraman V, eIA Jundi B, Warrant EJ, Byrne MJ, Khaldy L, et al. The insect central complex. Curr Biol. 2016; 26(11):R4537. doi: 10.1016/j.cub.2016.04.006 PMID: 27269718
- [5] Givon, L. E., Lazar, A. A., Yeh, C. H. (2017). Generating Executable Models of the Drosophila Central Complex. Frontiers in behavioral neuroscience, 11, 102. doi:10.3389/fnbeh.2017.00102